RESEARCH ARTICLE

BATTERY ENERGY WILEY

Comparison of lithium-ion battery cell technologies applied in the regenerative braking system

Mian Hammad Nazir[1] | **Abdulla Rahil[2]** | **Eduard Partenie[2]** | **Mark Bowkett[2]** | **Zulfiqar A. Khan[3]** | **Muhammad M. Hussain[1]** | **Syed Zohaib J. Zaidi[4,5]**

[1]Department of Electrical and Electronics Engineering, University of South Wales, Treforest, UK

[2]Faculty of Computing, Engineering and Sciences. Centre of Automotive Power System Engineering (CAPSE), University of South Wales, Treforest, UK

[3]Department of Design & Engineering, NanoCorr, Energy and Modelling (NCEM) Research Group, Bournemouth University, Poole, UK

[4]Institute of Chemical Engineering and Technology, University of Punjab, Lahore, Pakistan

[5]Laboratory for Energy Water and Healthcare Technologies, University of Punjab, Lahore, Pakistan

Correspondence

Mian Hammad Nazir, Department of Electrical and Electronics Engineering, University of South Wales, CF37 1DL, Treforest, UK.
Email: hammad.nazir@southwales.ac.uk

Abstract

This research presents the performance evaluation of four various types of top-of-the-line commercial and prototype lithium-ion energy storage technologies with an objective to find out the optimal cell technology, which is suitable for the development of high power battery packs for regenerative braking systems applied in next-generation demonstrator platform vehicles. The novel porotype lithium-ion cell technology is developed using linear combined nanofibers and microfibers battery separators laden utilizing wet nonwoven processes compared to the dry process laden multilayered porous film separators in commercial cell technologies. The performance comparison of all technologies has been conducted both at "cell-level" and "pack level" through the study of internal performance parameters, such as capacity, resistance, self-discharge, and battery temperature rise. This study also encompasses the differences in using external pack assembly and/or development parameters like the number of cells which are required to develop the pack, pack mass, pack volume, and pack cost. Both the internal performance parameters and external pack assembly and development parameters have revealed that novel prototype cell technology is the most optimal technology among all four cell technologies for regenerative braking systems, which have been investigated during this research. The novelty of this work is the development of novel prototype cell technology and its performance comparison with commercially available cell technologies used in regenerative braking systems of the latest hybrid/electric vehicles, which is in line with global initiatives, such as UK/EU transition to EVs and UN sustainability goals. The significance of this work in terms of high power pack development for regenerative braking of next-generation vehicles is evident from various industrial applications. This work will influence decisions for both battery testing techniques and accurate battery comparison methods for

automotive, locomotive, aerospace, battery manufacturers, and wind turbine industries.

1 | INTRODUCTION

Lithium-ion battery manufacturers around the globe use various techniques to improve the performance of batteries in terms of power, energy, storage losses, and extended useful temperature range.[1] This is achieved by either enhancing the quality of electrolyte additives, improving the materials chemistry of cell electrodes, and/or oxidation–reduction (redox) reactions.[2–4] Therefore, the performance of lithium-ion batteries directly relates to their internal chemistry.

Latest lithium-ion batteries age due to continuous cycling, high current operation, and self-discharge when left idle for longer durations.[5,6] One key reason for aging is internal capacity loss and internal resistance increase.[7] In addition to the above-aging factor, another factor like pack assembly/development, greatly influences important performance parameters like lifetime, cyclability, safety, and—most of all—cost.[8–15]

The project requirement was the development of a high power battery pack for a regenerative braking system (RBS) intended to integrate with the next-generation demonstrator platform vehicle for our lead partner. In the past few years, a lot of research has been conducted on the failure analyses of materials used in electrochemical battery cells.[16–37] In this project, a comparison of several competing lithium-based technologies at both cell and pack levels was performed. This involved the comparison of four different types of top-of-the-line commercial and prototype lithium cells manufactured by world-leading battery manufacturers and then selecting the optimal cell technology for the development of the next-generation high-power battery pack for RBS.[38,39] Regenerative braking can improve energy usage efficiency and can also extend the driving distance of hybrid/electric vehicles. This can improve the battery efficiency by 16%–25%, depending on the speed and the motor size.[40] The power dissipated by the vehicles can be partially taken back for powering up some of the utilities on board. Regenerative braking power generation could provide a remarkable power source for vehicles, but the amount of energy captured during braking considerably depends on the efficiency of the lithium-ion battery pack.

The comparison was conducted at both cell and pack levels according to IEC 62660-1 standard test procedures and conditions to test benchmark performance characteristics of lithium-ion technology. The main performance parameters that characterize the lithium-ion cell technology for their suitability in RBS involve internal parameters, such as capacity, resistance, self-discharge, and battery temperature rise, which have been considered in this research.[13,41,42] In addition, the pack level comparison was also performed by first developing the packs using the respective cell technologies and then comparing their performance using various electrical tests. The performance of assembled packs significantly depends on external pack assembly/development parameters, including series/parallel connections, the number of cells used in the assembly, weight, volume, and so forth, which is the motive of performing pack level performance comparison in this research. The cost-effectiveness of the developed pack was also considered a primary factor in selecting the optimized lithium-ion cell technology.

RBS promises significant gains in town driving as 62.5% of energy is dissipated in the metropolitan cycle due to frequent braking. If all braking energy could be regenerated with no loss in the regenerative system, fuel consumption would be improved by 33%.[43,44] Alternative sources state that the addition of regenerative battery storage systems to motor vehicles can achieve theoretical fuel savings of up to 23% in a 1600 kg vehicle on a level road urban driving schedule.[45,46] Therefore, battery technology used in RBS should be very efficient to take a large amount and rapid charge in a very short period. The novel prototype battery cell technology presented in this paper is capable of addressing these challenges.

This research has employed state-of-the-art techniques to develop a novel prototype pack. This newly developed prototype has major significance in essence that, unlike the conventional battery, it is capable of taking a substantial charge (up to 50% of braking energy) very quickly when vehicle brakes are applied, in turn, they can be charged at high currents (up to 600 A per cell). This energy, which would have otherwise been lost, is stored in the prototype pack and will be delivered back to the vehicle motors again, which will provide the energy to accelerate. Hence major energy recovery gains

are to be made and will result in substantial cost savings and battery charging time. Such packs do not act as the primary source of power, they only work in combination with the other main energy source, such as hydrogen fuel cells or electric vehicle batteries.[47]

Therefore, the research goal was to compare the novel porotype cell technology with the commercially available cell technologies used in RBS to find the suitability of prototype cell technology for the high power pack development, which is capable of taking huge charge in a very short period during regenerative braking of vehicles.

2 | TEST PROCEDURES

2.1 | Lithium-ion cells and test equipment

In this research, a comparative performance analysis was conducted on three commercially available and one novel prototype high power lithium-ion cell technologies for sustainability in RBS. The three commercially available cell technologies are widely used in the automotive sector for high-power applications including RBS, while the prototype high-power cell technology has been developed for RBS in super sports vehicles and is still in the testing phase. In all four cell technologies, an insertion material coke-type carbon substance, graphite anode was used with lithium cobalt oxides (LCO) as cathode material.[48] However, all these cells differ in the structure of the separator. The performance of lithium-ion batteries is greatly affected by the structure of the separators.[49] The porotype cell presented in this paper used the wet process laden nonwoven nanofibers and microfibers separator,[50,51] while the commercially available cells used the dry process laden nanoporous multilayered separators.[52,53] Many research articles have analyzed that wet process laden nonwoven mat separators perform better in high power batteries compared to dry process laden multilayered separators[54,55] (Figure 1).
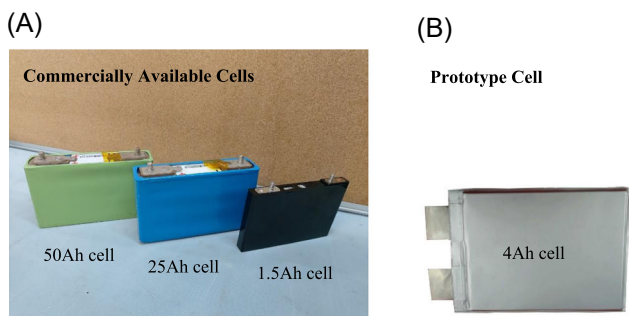

FIGURE 1 (A) Commercially available cells versus (B) prototype cell

Following cell technologies based on separator types have been analyzed in this research.*

Commercially available cell technologies—utilize dry process multilayered porous film separators:

- The 50 Amp-hours (Ah) cells use a dry process laden multilayered polypropylene-based microporous separator.[56]
- The 25 Ah cells use a modified dry process laden multilayered polypropylene-based microporous separator.[56]
- The 1.5 Ah cells use a dry process laden multilayered microporous separator-coated polypropylene (PP, Celgard 3501) and cellulose-based TF40-30 (NKK Nippon Kodoshi Corp.)[57,58]; and finally.

Prototype cell technology—utilize nonwoven processes mat separator:

- The 4 Ah cells utilize separator-coated poly(viylidene fluoride) (PVDF) that applies novel nonwoven wet processes laden nanofiber technology and its precision stamping technologies.[59] This cell features size and capacity comparable to that of the above commercial cells and realizes the same output density and durability as capacitors, which makes it a good candidate in the league of high-power automotive cells.

Commercially available versus prototype cell technologies:

In commercially available cell technologies, the stretched dry process laden multilayered porous film separators are thin, strong, and provide a good barrier between electrodes, but at the cost of having very high internal resistance and low ionic flow due to low porosity and high "dead space" that comes from starting with solid material and trying to impart porosity thereby resulting in cell power loss.[60] The prototype cell technology uses an alternative approach, where linear nanofibers and microfibers are combined in wet laid nonwoven processes to give separators that are strong and thin but have higher porosity (60%–70%) and so have much higher ionic flow. Figure 2 shows scanning electron microscope (SEM) images of separators extracted from fresh cells, clearly showing the porosity differences between the dry process laden multilayered and nonwoven wet process laden separators from fresh cells.

The specifications of the four cells are shown in Table 1. The focus of this research is on performance comparison of the above cell technologies using electrical testing, checking the suitability of the prototype cell, and finding the best technology for pack development for RBS application; however, the in-detailed manufacturing details of the porotype cell can be found in Liu et al.[61]

From here onward, we will refer to the cells by their respective Ah ratings, for example, a cell with a capacity of 50 Ah will be referred to as a 50 Ah cell.

2.1.1 | Preparations for cell-level testing

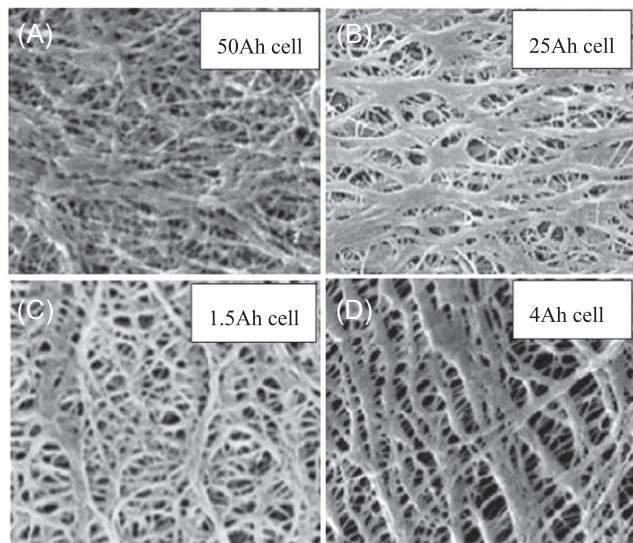A Bitrode MCV EV/HEV battery cell tester (Bitrode Corporation)[62] test bench was used for cell testing as

FIGURE 2 The schematic shows SEM images of separators extracted from fresh dry process laden commercially available (A) 50 Ah (B) 25 Ah (C) 1.5 Ah, and (D) fresh nonwoven wet process laden novel prototype 4 Ah cell.

shown in Figure 3A. It provides eight channels with current and voltage ranging from $1\,\mu A$–2400 A and 0–18 V, respectively, with an accuracy of $\pm 0.1\%$ full-scale. The above cells were installed in the environmental chamber as shown in Figure 3B. The test conditions were controlled using VisualCN software (Figure 3C), which was also used to constantly monitor the performance and was linked with Bitrode MCV EV/HEV battery cell tester. For cell level testing, no battery management system (BMS) was used, rather, current and voltage readings were directly taken from the terminal leads attached to the cell terminal, and PT100 temperature sensors installed on the terminal measured the cell temperature. These measurements were fed into Bitrode, which eventually controlled the charging/discharging of cells while keeping the cells within safe operating limits. For prismatic cells, a clamping device was used to keep cells upright (Figure 4A–C), while for pouch cells, a specialized jig was set up to safely assemble cells onto the jig before they were installed in the chamber (Figure 4D).

2.1.2 | Preparations for pack level testing

For pack level tests, the pack configuration of assembled packs from various cell technologies was based on the pack requirements from our project lead partner, that is, pack capacity = 0.67 kWh (=2.4 MJ), $V_{\text{min(pack)}} = 70$ V, $V_{\text{max(pack)}} = 120$ V. To address these pack requirements,

TABLE 1 Tables of specifications for 50, 25, 1.5, and 4 Ah cells

Cell specification				
Cell availability	**Commercially available cells**			**Prototype cell**
Cell technol	**50 Ah**	**25 Ah**	**1.5 Ah**	**4 Ah**
Format	Prismatic	Prismatic	Prismatic	Pouch
Type	Power/energy	Power	Power	Power
Cell chemistry	LCO	LCO	LCO	LCO
Rated capacity (C_0, Ah)	50	25	1.5	4
Maximum charge voltage (V_{max}, V)	4.1	4.15	3.8	4.2
Minimum discharge voltage (V_{min}, V)	2.75	2.75	2.2	2.7
Minimum operating temperature (T_{min}, °C)	−20	−30	−30	25
Maximum operating temperature (T_{max}, °C)	60	60	70	75
Maximum rated charging current ($I_{\text{chrg,max}}$, A)	125	600	600	600
Maximum rated discharge current ($I_{\text{dchrg,max}}$, A)	300	600	600	600
Weight (kg)	1.65	1.65	0.32	0.27
Dimensions (mm)	$171 \times 44 \times 111$	$171 \times 44 \times 111$	$180 \times 10.9 \times 126$	$160 \times 6.4 \times 257$

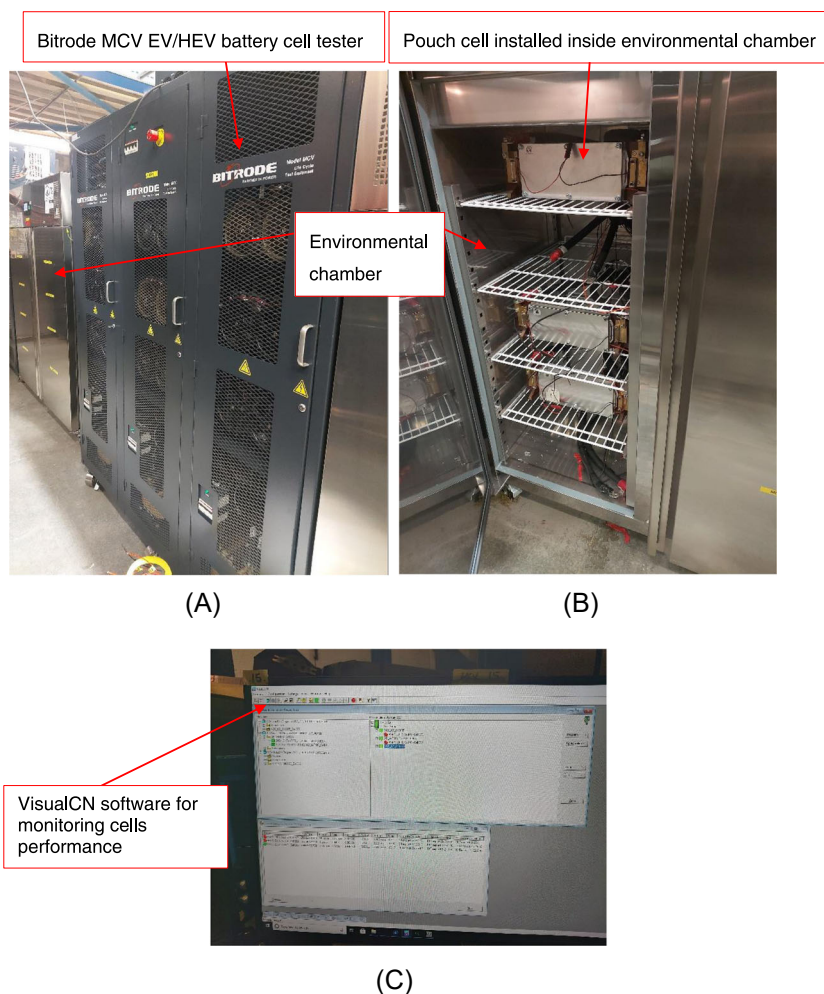Abbreviation: LCO, lithium cobalt oxides.

FIGURE 3 The schematic shows (A) a Bitrode MCV EV/HEV battery cell tester, (B) an environmental chamber for performing cell testing under controlled conditions, and (C) VisualCN software for controlling test conditions and constantly monitoring the performance of cells.

the pack configuration for 25 Ah cell was set as 1p × 30s, for 4 Ah cell as 2p × 30s, and for 1.5 Ah cell as 4p × 30s. For illustration, 25 Ah (1p × 30s), 1.5 Ah (4p × 30s), and 4 Ah (2p × 30s) 0.67 KWh packs are shown in Figure 5.

In pack assembly, the stiffness of the prismatic cells is regarded as better compared to pouch cells, which are produced with the help of a flat winding, and then inserted into a solid housing. However, with the pouch cell, the stiffness is not given by the pouch foil and must be supplemented with a frame when inserted into the pack casing. The cells are stored in a casing to provide them mechanical support. The pack casing is made of aluminum. Furthermore, the cells are connected on the tabs by busbars made of aluminum. For temperature, PT100 sensors are applied to the tabs of cells. Unlike cell level testing, for pack level tests, each battery pack had its individual BMS (REAP BMS), which was responsible for opening and closing contactors during charging/discharging and looking after the battery's overall safety

performance, including temperature, current, and voltage levels. The pack performance during testing was constantly monitored by Bitrode MCV VisualCN software using controller area network (CAN) messages from BMS.

In this research, for thermal management, no cooling method was introduced in pack assembly, which is a part of our forthcoming study.

2.2 | Test methodology

In total, six types of tests were performed to compare the performance of four cell technologies. All these tests followed the international standard IEC 62660-1 procedure.[63] The C-rate/current rating and temperatures corresponding to each test are mentioned in Table 2. Furthermore, for repeatability, all six tests were repeated three times each to ensure the accuracy of the results.
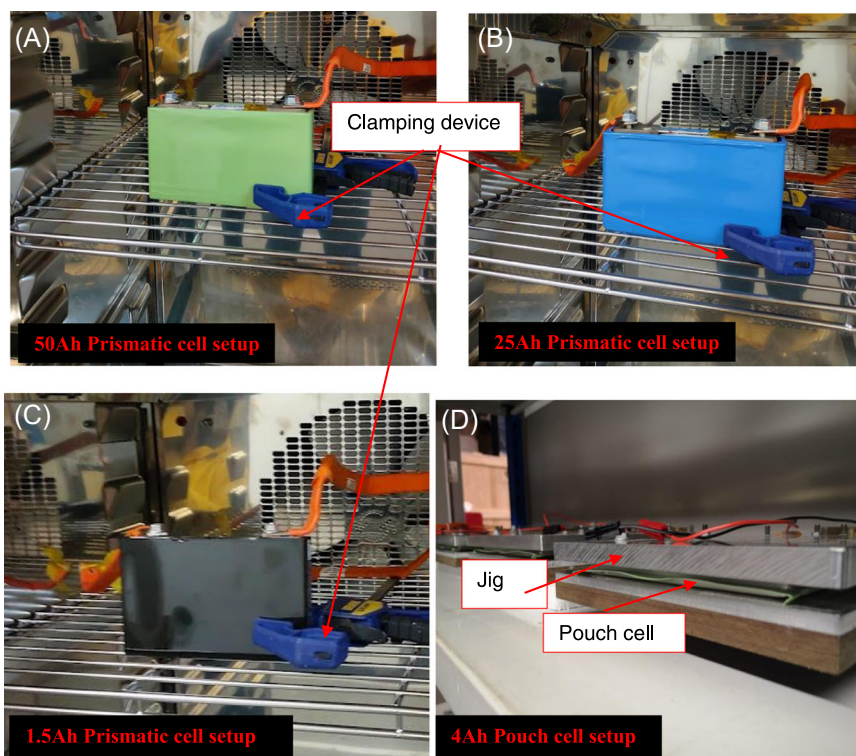
FIGURE 4 The schematics show the installed (A) 50 Ah (B) 25 Ah (C) 1.5 Ah prismatic cells and (D) 4 Ah pouch cell on a specialized jig installed inside an environmental chamber connected to Bitrode MCV EV/HEV battery cell tester for cell level testing.

The hierarchy in which tests were performed is shown in Table 2. This table clearly indicates that Tests 1–3 were performed at the cell level, while Tests 4–6 were performed at the pack level. The tests included cell level capacity retention, cell level high power pulse characterization (HPPC), cell level self-discharge Test 3, pack level capacity retention Test 4, pack level cyclic aging Test 5, and finally, pack level real-world drive cycles Test 6.

The tests were performed in a fashion to sequentially filter the best cell technology suitable for high-power applications. The horizontal filtration chart is shown in Figure 6, illustrating the hierarchy in which cells were filtered out during testing. The chart explains the test hierarchy for the filtration of cells.

It can be seen in Figure 6 that Test 1 was performed on all four cell technologies. The results from Test 1 were compared to filter the cell technologies, which can go for further testing. Three out of four cells were filtered for the next Tests 2 and 3. Tests 2 and 3 were performed to compare the cell level performance of three respective filtered cells, while Test 4 was performed to compare the pack level performance of three filtered cells. For pack level performance in Test 4, three packs each 0.67 KWh (packs energy calculations already discussed) were developed using three respective filtered cells. The reason for comparing pack level performance of three cell technologies in Test 4 was to get clarity on pack level

performance of all three cell technologies before further filtration. After pack level performance Test 4, two out of three cell technologies were filtered for further Test 5. Test 5 revealed the best fit cell technology, which was finally subjected to a real-world drive scenario in Test 6.

2.2.1 | Cell level tests

The cell level capacity retention Test 1

It was performed to determine an accurate and comparable capacity retained by cells at 25°C when they were cycled for 5000 reference cycles at various C-rates, that is, 1 C, 4 C, and MaxC.[64] Where one reference cycle indicates a complete chare-discharge cycle and MaxC indicates the maximum rated charge $I_{chrg,max}$ and discharge $I_{dchrg,Max}$ currents of cells as mentioned in Table 1. Such that for various C-rates during the charge cycle, the constant current charged the cells up to V_{max}, and maintained a constant voltage of V_{max} until the current ramped down to $0.05 \times$ rated capacity (in Ah). Likewise, during the discharge cycle, the constant current discharged the cells to V_{min} and maintained constant V_{min} until the current ramped up to $0.05 \times$ rated capacity. There was a rest time of 1 h in between charge and discharge cycles to allow cells to return to electrochemical and thermal equilibrium conditions. To observe
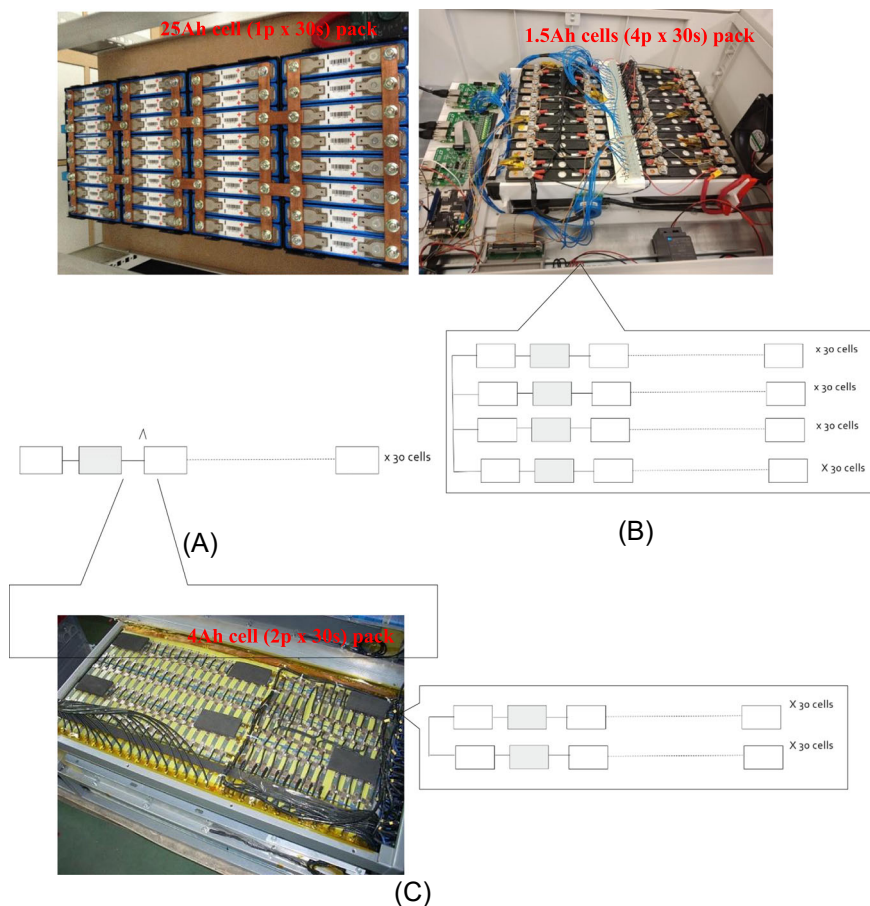
FIGURE 5 The schematics show 0.67 kWh packs assembled using (A) 25 Ah cell (1p × 30s), (B) 1.5 Ah cells (4p × 30s), and (C) 4 Ah cells (2p × 30s) for pack level testing.

TABLE 2 List of tests performed with their corresponding test conditions

Type of testing		C-rates/current	Temperature set
Cell level tests			
Test 1	Cell level capacity retention	1 C, 4 C, MaxC	25°C
Test 2	Cell level high power pulse characterization (HPPC)	100 A constant discharge current	25°C
Test 3	Cell level self-discharge	-	25°C and 45°C
Pack level tests			
Test 4	Pack level capacity retention	200, 600 A constant charge–discharge current	25°C
Test 5	Pack level cyclic aging	50 A constant continuous reference cycles	25°C
Test 6	Pack level real-world drive cycles	Continuous varying power as per drive cycle profile	25°C
		Profiles max power during charging: 1800 W	
		Profiles max power during discharging: 2100 W	

the rise in temperature of all four cell technologies as a function of reference cycles, a special constant current capacity test was designed with charge–discharge cycles at a constant 100 A current corresponding to reference cycles. The reason for the constant current capacity test was to make a fair comparison between cells to address temperature rise. The cycles were repeated three times.
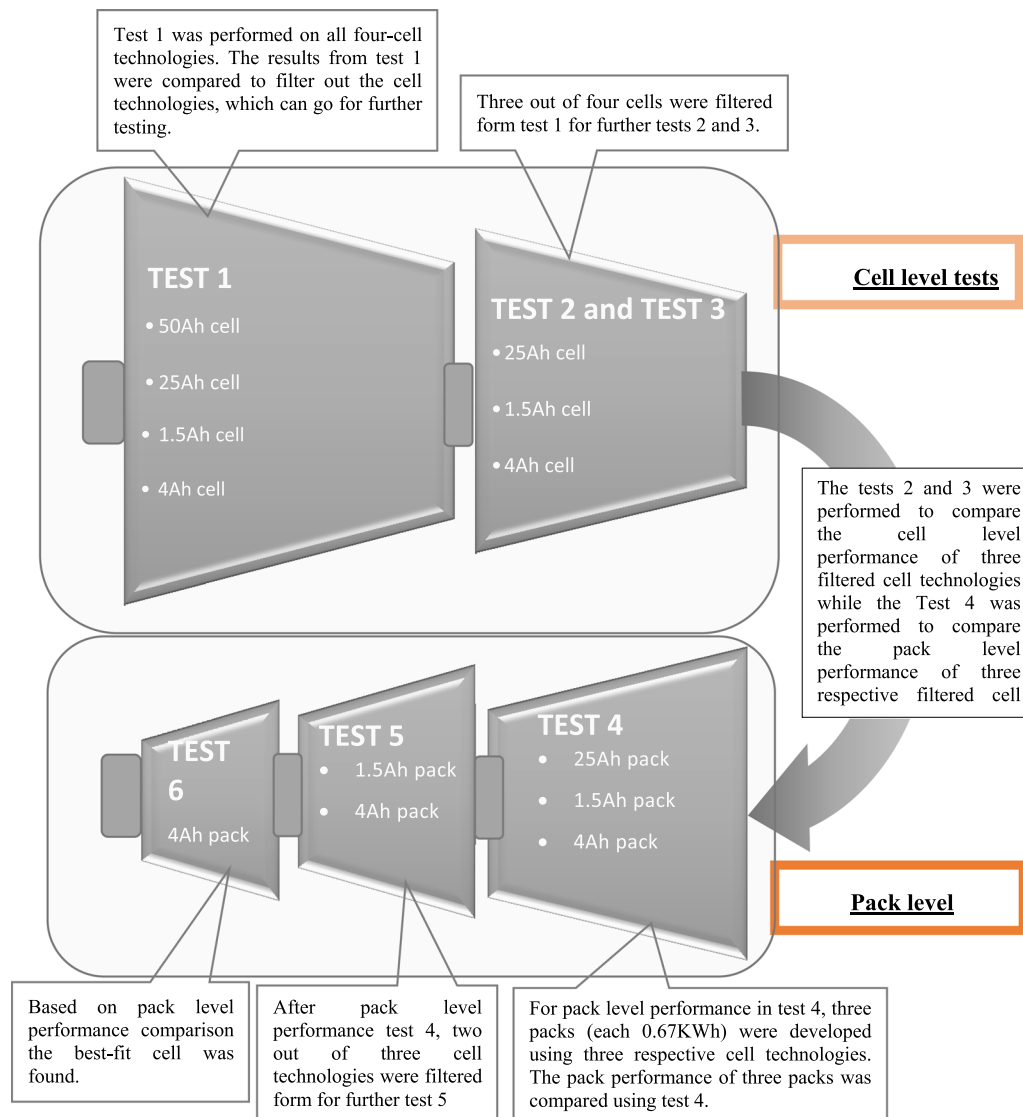
FIGURE 6 Horizontal filtration chart showing test procedure performed in a fashion to sequentially filter out the best cell technology suitable for high power applications.

The cell level HPPC Test 2

It was performed to determine the internal DC resistance and dynamic power capability of cells at various state of charges (SOCs) (from 100% SOC to 20% SOC) at 25°C. In the HPPC test, single repetitions of profile separated by 20% SOC constant discharge segments, each followed by ½ h rest period were performed.[65] The test initially started from 100% SOC and ended after completing the final profile at 20% SOC, and final ½ h rest. The pulse tests were designed to estimate the DC internal resistance of the cells at a given temperature and SOC.

The cell level self-discharge Test 3

It was performed at 25°C and 45°C to validate the capacity loss of cells independent of charge–discharge cycling, that is, under long-term storage conditions.[66] Before going to storage conditions, the candidate cells

were fully charged to 100% SOC at 1 C. The cells were then stored in an open-circuit condition for 3 months in preconditioned environmental chambers at 25°C and 45°C. The voltage and temperature values during storage time were continuously logged to dataTaker DT85 smart data logger equipment[67] with a sampling rate of 3 min/sample. All measurement devices except the data logger were disconnected from the cells during this period to reduce parasitic losses.

2.2.2 | Pack level tests

The pack level capacity retention Test 4

It was performed on 0.67 KWh packs in which pack level capacity performance comparison of cell technologies was simulated for two constant current scenarios: that is,

at 200 and 600 A. The pack capacity retention was demonstrated in terms of the ability of the pack to retain stored energy at the abovementioned two current levels. The reason for selecting 200 and 600 A current is that in a hybrid electric vehicle's RBS, the 200 A relates to energy captured in the pack under normal braking while 600 A relates to energy captured under extreme braking, for example, when going downhill. The pack level test followed the standard capacity test procedure with charge–discharge cycles and a 1-h rest in between both cycles.

The pack level cyclic aging Test 5

It was performed to determine cells capacity loss, temperature rise, and internal DC resistance increase over repeated standardized cycles until the criteria for the end of life was reached, namely a capacity loss of 20% and/or a resistance rise of 100%.[68] The charge–discharge cycle was conducted at 4 C and repeated for 6000 reference cycles at 25°C without rest between charge and discharge. Internal DC resistance of cells was calculated using capacity loss, voltage drop, and OCV.[69]

The pack level real-world drive cycle Test 6

It was performed to validate the performance of candidate cell technologies against a real-world drive cycle profile, specific to the intended application for example in-city charge–discharge automotive cycle.[70] The profile was pack power in Watts and was repeated three times continuously. This test was specially designed to analyze the rise in temperature of packs subjected to continuous real-world profiles.

For all tests, the raw data from Bitrode was logged in excel format and further analysis was performed using the MATLAB program to extract and plot the required information.

3 | RESULTS AND DISCUSSION

3.1 | Test 1—The cell level capacity retention

Figure 7 shows that the charge data capacity loss is significantly dependent on the charge rate. At high constant-current C-rates, the capacity loss was considerably higher than for low C-rates. The loss in cell capacity during the charging phase of a total of 5000 reference cycles showed that as the current for respective cell technology was increased from 1 C to MaxC there was a significant loss of capacity for all cell technologies. Where values for MaxC current during charging and discharging for all four cell technologies are shown in
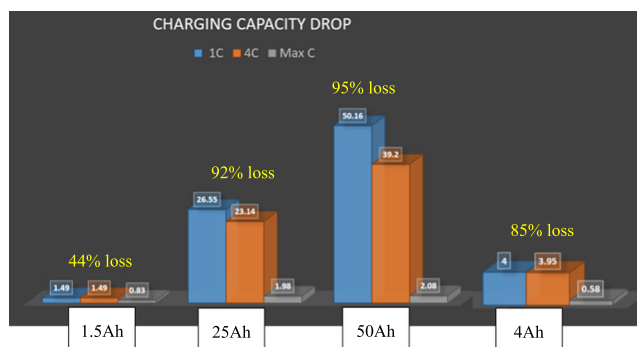

FIGURE 7 The loss in capacity at 1 C, 4 C, and MaxC for various cells during the charging phase
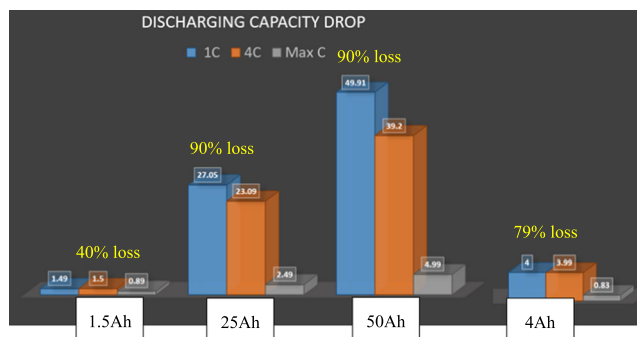

FIGURE 8 The loss in capacity at 1 C, 4 C, and MaxC for various cells during the discharging phase

Table 1 across maximum rated charging current $I_{chrg,max}$ and maximum rated discharging current $I_{dchrg,max}$, respectively. The maximum loss in capacity was observed for 50 Ah cell (95%) followed by 25 Ah (92%), 4 Ah (85%), and 1.5 Ah (44%) cells.

Likewise, during the discharging phase, the maximum loss in capacity was observed for 50 Ah cell (90%) followed by 25 Ah (90%), 4 Ah (79%), and 1.5 Ah (40%) cells, as shown in Figure 8.

The capacity retention test also showed a decline in specific energy for all cell technologies as a function of specific power when C-rate was increased from 1 C to MaxC, as shown in Figure 9. The following graph shows specific energy vs specific power trends at various C-rates (1 C, 4 C, and MaxC) during the discharge phase. The graph shows that for the 50 Ah cell when C-rate was increased from 1 C to MaxC, the trend exhibited the sharpest dip in specific energy compared to other cells. It is well-known that specific energy (Wh/kg) is a function of cell capacity (Ah), cell voltage (V), and per unit mass (kg).[71] As from Figures 7 and 8, it is evident that for both charge and discharge phases, the maximum capacity loss was observed for 50 Ah cells. This large capacity loss of 50 Ah cell also resulted in a sharp dip in specific energy
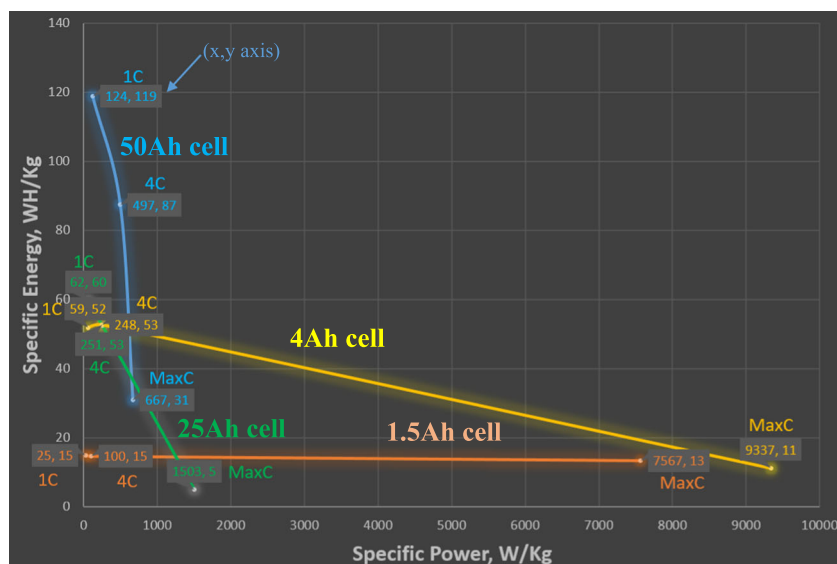
FIGURE 9 Specific energy versus specific power for 50, 25, 4, and 1.5 Ah cells at various C-rates during the discharge phase: 1 C, 4 C, and MaxC
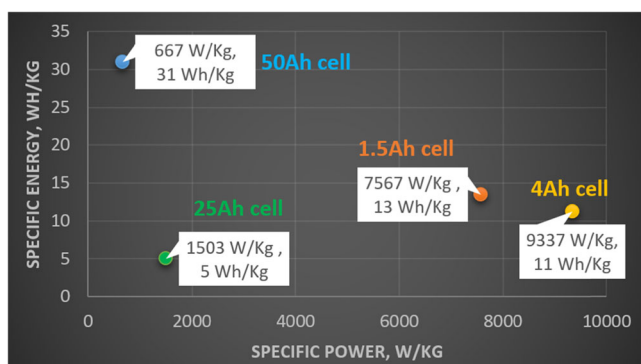

FIGURE 10 Specific energy versus specific power for 50, 25, 1.5, and 4 Ah at MaxC only during the discharge phase.

trends in Figure 9 due to the reason that specific energy is a function of capacity, as discussed above. Likewise, the sharpness of dips for trends decreased in the following order, that is, 25, 4, and 1.5 Ah cells, respectively, such that the trend for the 1.5 Ah cell was almost a horizontal line. This horizontal line is an indication that the 1.5 Ah cell brilliantly retains specific energy with increasing C-rate, possibly due to advanced lithium-ion capacitor technology. However, overall, in terms of high power delivery, which is also the research question of this project, the 4 Ah cell proved much better compared to the other three technologies.

For more clarity, the bubble plot in Figure 10 showed the maximum power delivery performance of cell technologies at MaxC. The plot shows an interesting observation that although the 4 Ah cell delivered the highest power, the downside with this technology is that

it was not able to retain specific energy at MaxC, unlike the 1.5 Ah cell. Likewise, 25 Ah cell performance was not the best in terms of power delivery, but still better compared to 50 Ah cell.

A constant current capacity retention test at 100 A was performed to address the rise in temperature for all four cell technologies as a function of 5000 reference cycles as shown in Figure 11. The results showed that the highest rise in temperature was observed for 50 Ah cells followed by 25, 1.5, and 4 Ah cells. Such a large temperature rise of 50 Ah cell can accelerate the degradation of cell, especially when subjected to applications with high current ratings.

Therefore, the cell level capacity retention Test 1 concluded that 50 Ah cell technology did not prove to be a good choice for high power applications and was not taken forward for further testing in this research.

3.2 | Test 2—The cell level HPPC

Figure 12 shows the trends for internal DC resistance of three cell technologies (25, 4, and 1.5 Ah) from 100% to 20% SOC. For a fair comparison, the HPPC test was performed at constant discharge segments of 10 A for all cell technologies. Overall performance in terms of internal DC resistance showed that the highest resistance was observed for 25 Ah cells followed by 1.5 and 4 Ah cells. High internal DC resistance results in restricted current, voltage drops on load, and cells heat up, while cells with low internal DC resistance deliver high current on demand.[72]
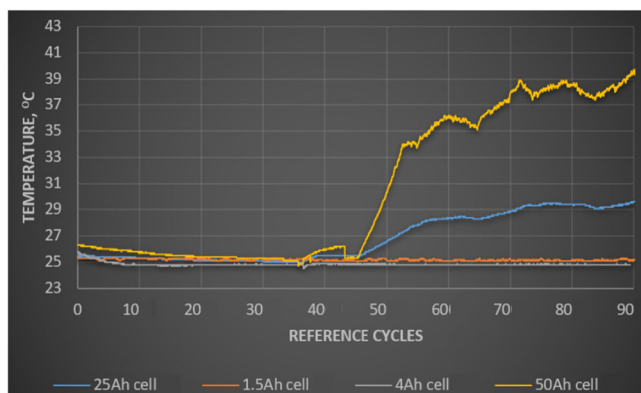
FIGURE 11 Temperature as a function of reference cycles for 50, 25, 1.5, and 4 Ah at a constant current of 100 A
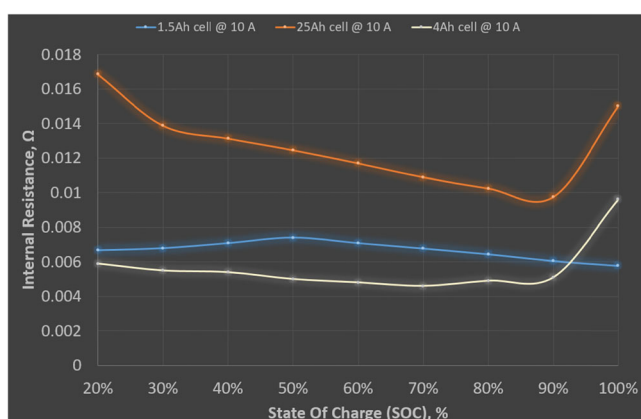

FIGURE 12 Comparison of internal DC resistance of 25, 4, and 1.5 Ah cells by using high power pulse characterization test

Another important observation was that at two extreme SOCs, that is, at 20% and 100%, the 25 and 4 Ah cells showed the largest resistance. However, unlike 25 and 4 Ah cells, the 1.5 Ah cell showed opposite behavior, that is, it had the lowest resistance at two extreme SOCs. This distinct behavior of 1.5 Ah compliments the results from Barai and colleagues.[73,74] In general, lower number of available Li sites in the cathode as the cell approaches either extremes of SOC in lithium-ion technology, such as 25 and 4 Ah cells, the resistance in the low SOC region is higher, and internal DC resistance at high SOC also increases.[75,76] In contrast, lithium-ion capacitor, that is, 1.5 Ah cell tends to show low resistance at both extremes of SOC probably because of the internal chemistry of these cells, which also resembles the internal DC resistance trends of supercapacitors as a function of SOC.[77]

Therefore, the HPPC test 2 concluded that 25 Ah cell technology did not perform well due to high internal DC resistance. Before filtering any technology, some other

tests were performed on all three cell technologies to further investigate their performance.

3.3 | Test 3—Cell level self-discharge

Self-discharge test at 45°C was performed for almost 3 months on all three cell technologies, that is, 25, 4, and 1.5 Ah cells, as shown in Figure 13. The most interesting result was found for the 4 Ah cell, which showed that at the end of the first month the cell discharged 87% of its initial voltage, well below the minimum voltage ($V_{min} = 2.7$ V), showing that the cell failed completely. The test was repeated for the second month with a fresh cell. This cell again showed similar behavior and discharged by 75% of its initial voltage, that is, it failed completely. To confirm this abnormal behavior, the test was repeated for the third month with fresh cells, which showed almost the same discharge behavior as the previous two. This severe drop in voltage for the 4 Ah cell shows that this cell might not be a good choice for applications that stay nonoperational for long durations at higher temperatures like 45°C. The other two cells, that is, 1.5 and 25 Ah discharged by 12% and 34%, respectively. The 25 Ah cell almost reached its minimum voltage ($V_{min} = 2.75$ V) at the end of the third month.

Self-discharge test at 25°C was performed for three consecutive months as shown in Figure 14. It was seen that the total drop in voltage for 4, 1.5, and 25 Ah cells during this period was 11%, 3%, and 5%, respectively. This showed that the 4 Ah cell performed much better at 25°C compared to 45°C, as this cell did not fail at 25°C. In addition, the performance of other cells was much better compared to their performance at 45°C. Overall comparison of the self-discharge test for all three cells showed that the 1.5 Ah cell performed better compared to the other two cell technologies as the voltage drop for
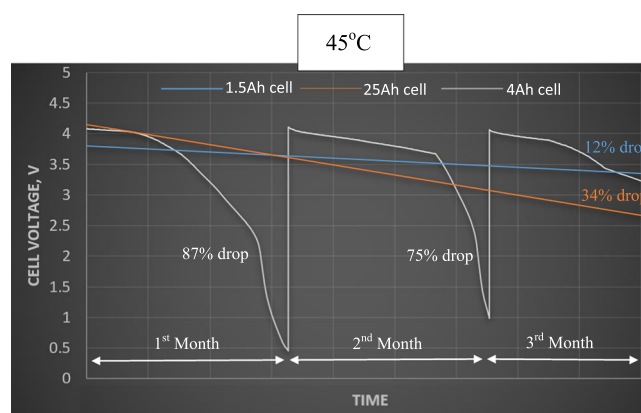

FIGURE 13 Self-discharge test of 4, 1.5, and 25 Ah cells at 45°C for three consecutive months
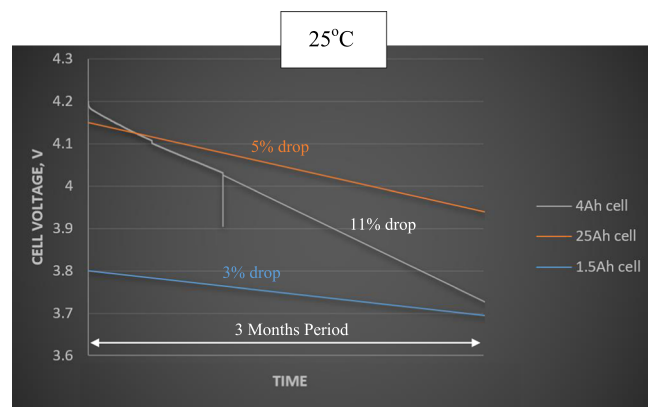
FIGURE 14 Self-discharge test of 4, 1.5, and 25 Ah cells at 25°C for three consecutive months

FIGURE 15 Pack level comparison for the loss in pack capacity from 200 to 600 A

the 1.5 Ah cell from initial voltage was only 12% and 3% at 45°C and 25°C, respectively.

It was difficult at this stage to filter any cell technology, although the 4 Ah cell did not perform well in terms of self-discharge; however, its performance in terms of power and energy delivery was far better compared to the other two cell technologies. Therefore, some other tests were performed for further comparison.

3.4 | Test 4—Pack level capacity retention

From here onwards, further comparative tests were performed at the pack level. The pack level capacity retention test was performed on all three cell technologies based on the test specifications discussed in the test procedures section. The pack capacity retention was demonstrated in terms of the ability of the pack to retain the stored energy at two current levels, that is, 200 and 600 A, as shown in Figure 15. The minimum loss in pack capacity was observed for the pack that was made of 4 Ah cells (referred to as for P-4 Ah pack) followed by P-1.5 and P-25 Ah packs. It is noteworthy that at 600 A the minimum loss in capacity was observed for the 4 Ah cell at the pack level compared to its capacity loss at the cell level (discussed in cell level capacity test Section 3.1). The reason is that the configuration of 4 Ah cells in a pack (2p × 30s) allows 4 Ah cells to operate at only 75 C compared to 150 C at the cell level.

Likewise, another observation from Figure 16 is that at 600 A, the P-1.5 Ah pack offered a high capacity loss compared to the P-4 Ah pack, while interestingly opposite behavior was observed for both at the cell level (discussed in Section 3.1), where 1.5 Ah cell offered a low capacity loss compared to 4 Ah cell. The reason is that 1.5 Ah cells at pack level (4p × 30s) operate at 80 C compared to 75 C for
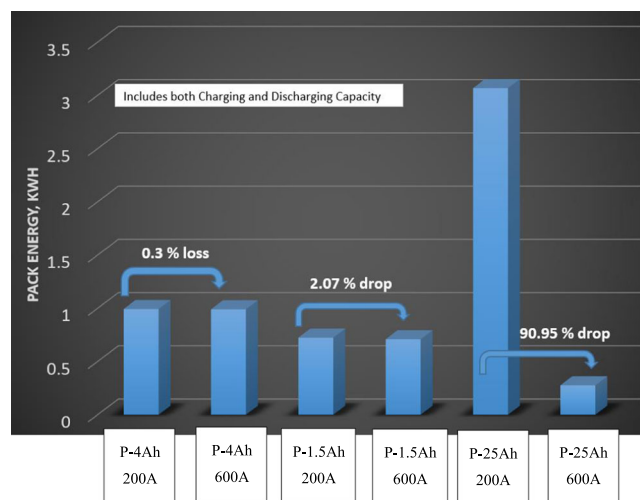
4 Ah cells at pack level (2p × 30s). Therefore, the comparison of the P-1.5 Ah pack with the P-4 Ah pack at 600 A showed that the P-4 Ah pack outperformed the P-1.5 Ah pack in terms of capacity retention.

As shown in Figure 10, it was observed that the P-4 Ah pack performed well in terms of both energy and power at both 200 and 600 A followed by the P-1.5 Ah pack. Comparatively, the P-25 Ah pack performed very well only in terms of energy at 200 A (with corresponding power almost the same as of other packs) but at 600 A the energy of the P-25 Ah pack dropped even below the minimum pack requirement (highlighted as a yellow area in Figure 10), that is, 15 KW and 2.4 MJ. Our project lead partner provided the minimum pack requirement. Therefore, the P-25 Ah pack did not prove to be a good choice for high power applications because at high current (600 A) the energy loss was significant making it unsuitable to be used as an energy storage system during extreme braking.

Furthermore, in Figure 17, P-4 and P-1.5 Ah packs showed good voltage retention during 1 h rest period between charge–discharge cycles and the voltage drop was not significant. Also for both packs, 200 and 600 A currents accounted for almost the same level of voltage drop during rest showing that these packs were able to maintain voltage even for higher currents. However, the P-25 Ah pack showed a significant drop in voltage when subjected to 600 A, showing that P-25 totally failed to retain voltage at higher currents.

As power delivery is of main concern in this study, the above tests concluded that 25 Ah cell technology did not prove to be a good choice for high power applications due to pack capacity loss and pack voltage drop at high current and high internal DC resistance. The 25 Ah cell
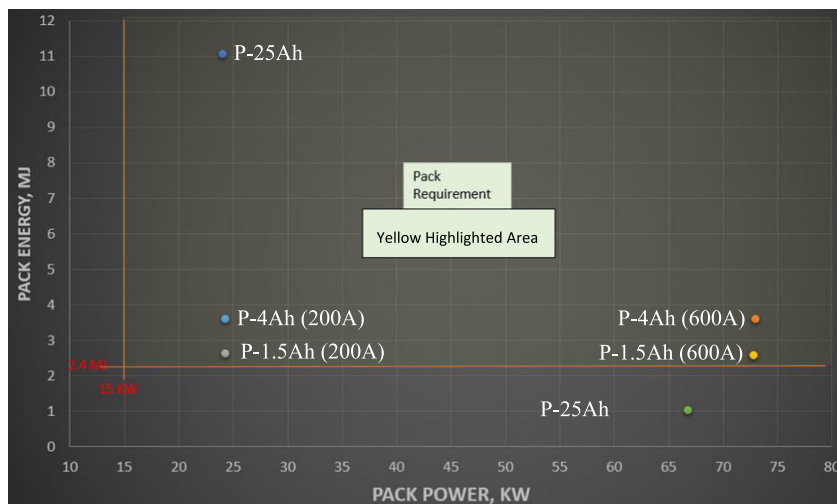
FIGURE 16 Pack level comparison of P-25, P-4, and P-1.5 Ah packs at 200 and 600 A
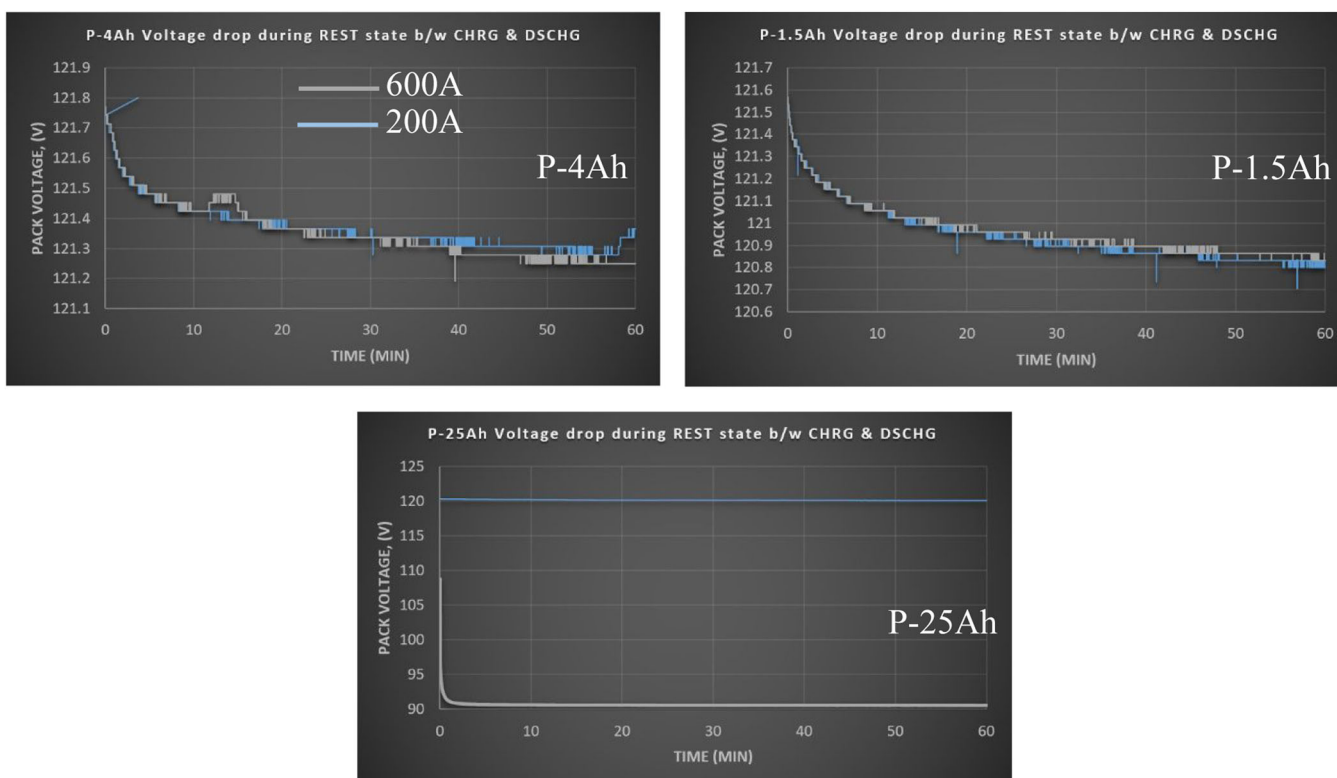

FIGURE 17 Comparison of voltage drop during rest period for P-4, P1.5, and P-25 Ah packs at 200 and 600 A

technology was not taken forward for further testing in this study.

However, in applications where self-discharge is of main concern, the 25 Ah cell technology can be taken into consideration as its self-discharge performance is good compared to the other two cell technologies.

The 4 and 1.5 Ah cell technologies, based on their good capacity and voltage retention, pack power delivery and internal DC resistance performances were taken for further tests.

3.5 | Test 5—Pack level cyclic aging

Figure 18A,B show capacity fade and cell temperature rise of P-4 and P-1.5 Ah packs, respectively when subjected to 6000 continuous reference cycles at 25°C and at 50 A without rest. The initial capacity of both packs was ~8 Ah. It can be seen that the P-4 Ah pack lost 10% of its initial capacity at the end of 6000 cycles with the rise in temperature from 25°C to 28°C. Compared to P-4 Ah, the P-1.5 Ah lost only 7% of its
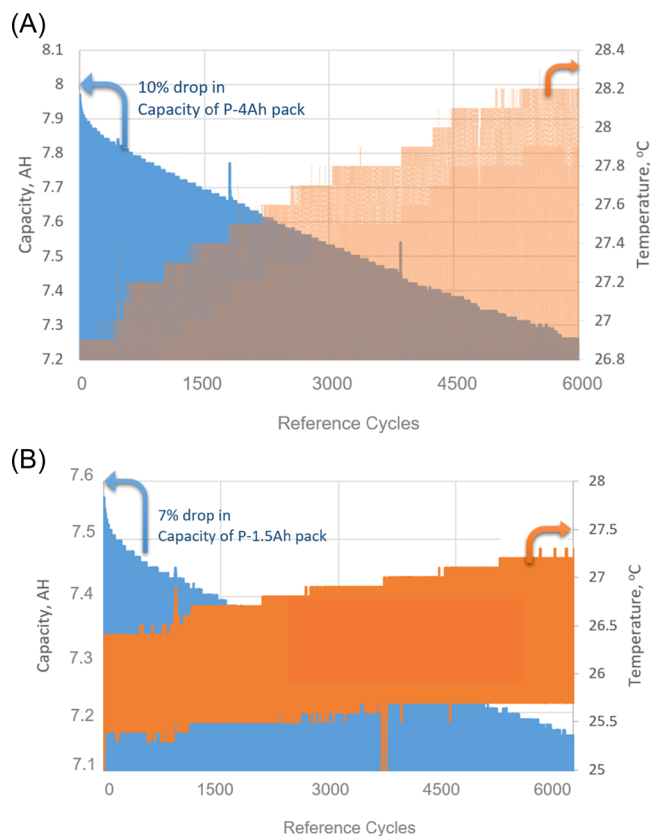
FIGURE 18 Drop in the capacity of (A) P-4 cell and (B) P-1.5 cell and rise in the corresponding temperature during 6000 continuous reference cycles.

FIGURE 19 Increase in internal DC resistance of P-4h and P-1.5 Ah cells during 6000 continuous reference cycles at 25°C and at 50 A.

initial capacity with the rise in temperature from 25°C to 27°C.

Continuous cycling also resulted in the internal DC resistance rise for P-4 and P-1.5 Ah packs as shown in Figure 19. A 2% and 1% rise in internal DC resistance was observed for P-4 and P-1.5 Ah packs, respectively. It is interesting to note that although overall internal DC resistance for P-1.5 Ah is high compared to the P-4 Ah pack but the rise in its initial resistance is only 1%, which is low compared to a 2% rise for the P-4 Ah pack. The reason for the overall high internal DC resistance of the P-1.5 Ah pack can be attributed to the internal chemistry of the 1.5 Ah cell; however, the low rise in resistance can be related to a low capacity drop during cycling, which is only a 7% drop of its initial capacity. According to Molaeimanesh et al.,[78] the cyclic aging capacity loss is due to the loss of active lithium, which also results in increased internal DC resistance and a rise in temperature of the pack.

Pack level capacity test showed that P-4 Ah pack is better than P-1.5 Ah pack in terms of capacity retention and voltage retention at high C-rates and pack power delivery; however, contrarily when it comes to cyclic aging, P-1.5 Ah pack is better than P-4 Ah pack because the cyclic capacity drop of P-1.5 Ah is low compared to P-4 Ah.
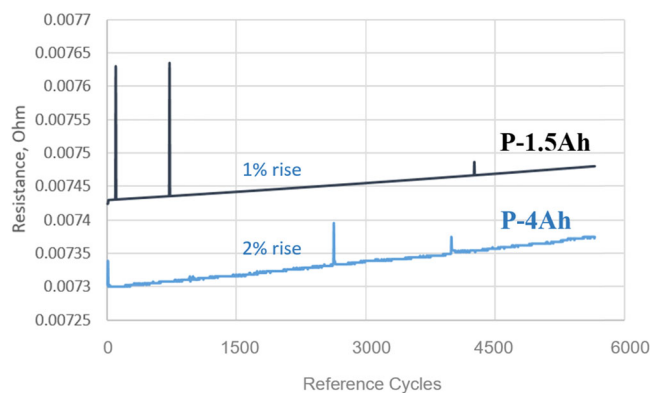
As both technologies have pros and cons, therefore, it is difficult to filter at this stage, and another test was performed to find the best fit.

3.6 | Test 6—Pack level real-world drive cycles

The temperature profiles for both packs, that is, P-4 and P-1.5 Ah correspond to the drive cycle pack power profile (in Watts) for three continuous cycles, as shown in Figure 20. Maximum power as per drive cycle profile was 1800 W during charging and 2100 W during discharging. The temperature profiles corresponding to power profiles showed that during this continuous in/out program, the temperature of P-4 and P-1.5 Ah packs reached a maximum value of 39°C and 30°C, respectively, and then stabilized with 2%–5% variation. The overall temperature of the P-4 Ah pack stayed higher throughout the profile compared to the P-1.5 Ah pack.

In previous Section 3.5, the pack level cyclic aging test showed the drop in temperature rise of P-4 Ah was higher compared to P-1.5 Ah during 6000 continuous cycles. Similar results were again observed in the drive cycle test, where the temperature rise of the P-4 Ah pack was higher compared to the P-1.5 Ah pack.

This shows that the temperature performance of the P-1.5 pack is better compared to the P-4 Ah pack.

4 | ABSTRACT LEVEL COMPARISON—CONCLUDING TABLE

Table 3 shows the abstract level comparison of all four cell technologies with various colors used for grading their performances compiling all the above results.
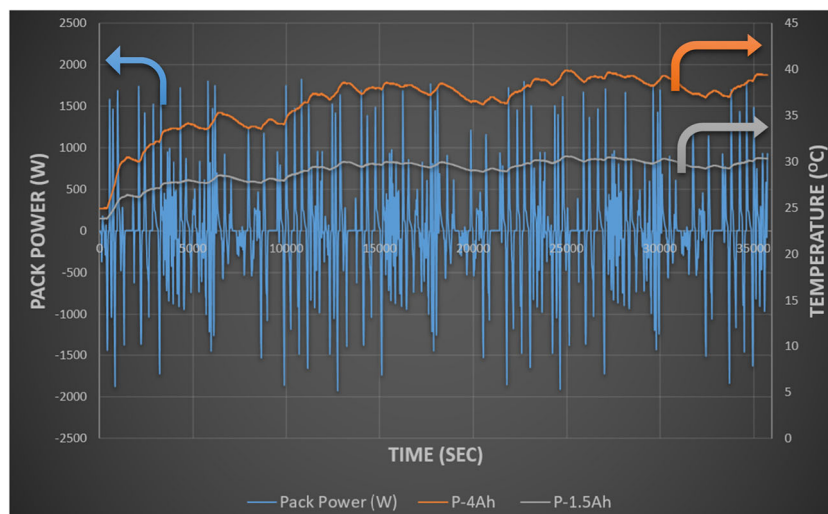
FIGURE 20 Real-world drive cycle result showing temperature profiles (in °C) of P-4 and P-1.5 Ah corresponding to pack power profile (in W) as a function of time (in s).

TABLE 3 Abstract level comparison of 50, 25, 1.5, and 4 Ah cells

Cells Type	Cell Specific Power @MaxC	Cell Capacity loss from 1C to MaxC	Per cell cost	Cells required for making a Pack	Pack Cost*	Pack Mass*	Pack Volume*	Pack Power @600A	Pack Capacity loss from 200A to 600A	HPPC-Cell Internal Resistance @50% SOC	Cell Self-Discharge (in 3 months) 25°C	Cell Self-Discharge (in 3 months) 45°C	Pack Capacity loss after 6000 cycles	Pack Resistance after 6000 cycles	Temperature rise during Drive Cycle test
50Ah cell	667Wh/Kg	95%	£200	30 Cells (1P x 30S)	£6000	50Kg / 1.65Kg per cell	21L	50Ah cell was not taken forward for these tests due to lowest cell power and cell capacity performance at MaxC							
25Ah cell	1503Wh/Kg	92%	£200	30 Cells (1P x 30S)	£6000	50Kg / 1.65Kg per cell	21L	1MJ	90%	12milliohm	5%	34%	25Ah cell was not taken forward for these tests due to lowest pack power, pack capacity and internal resistance performance		
1.5Ah cell	7567Wh/Kg	44%	£68	120 Cells (4P x 30S)	£8160	39Kg / 0.32 Kg per cell	27L	2.6MJ	2.0%	8milliohm	3%	12%	7%	7.5milliohm	30°C
4Ah cell	9337Wh/Kg	85%	£50	60 Cells (2P x 30S)	£2900	16Kg / 0.27 Kg per cell	19L	3.6MJ	0.3%	5milliohm	11%	87%	10%	7.3milliohm	39°C

▮ = Lowest performance

▮ = Low-Mid performance

▮ = Mid-High performance

▮ = Best performance

* Calculations based only on number of cells making a pack. These does not include thermal management, pack casing and electronics components

In addition to testing, other important pack development/assembly parameters were also considered, for example, (i) cost per cell, (ii) number of cells required to develop a pack, (iii) pack cost, (iv) pack mass, and (v) pack volume. In all these five parameters, 4 Ah cell technology outperformed (shown in green) except in one parameter, that is, the required number of cells for developing a pack. However, the required number of cells to develop a pack becomes "not-so-important," if the resulting

developed pack has low development cost, small mass, and small volume.

Further, 4 Ah cell technology outperformed in most of the tests (e.g., pack power, pack capacity retention from 200 to 600 A, cell internal resistance, etc.), as evident from most green boxes compared to other cell technologies. The only lowest test performance by 4 Ah cell technology was the self-discharge (shown in red). Therefore, 4 Ah cell technology due to its high self-discharge rate will not be suitable for applications with a long storage requirement.

In this research, power delivery, as well as pack development parameters, were of key interest. Self-discharge was of supplementary interest herein. Based on this interest, 4 Ah cell technology, after comprehensive comparison was graded as "The Best" technology for high power applications among all four. The other cell technologies were graded as: 1.5 Ah is better than 25 Ah is better than 50 Ah cell technology.

Therefore, as per the research goal, it was established that among all four technologies, 4 Ah cell technology is most suitable for the development of high power pack, which can be charged at high currents meaning that the pack is capable of taking huge charge in a very short amount of time during regenerative braking of vehicles.

5 | CONCLUSIONS

A comparison of four different types of top-of-the-line commercial and prototype lithium cells (4, 1.5, 25, and 50 Ah cells) was performed to find the optimal cell technology, which is suitable for the development of the next-generation high-power battery pack for RBS. The research has characterized both the internal performance parameters like capacity, resistance, self-discharge, and battery temperature rise and external pack assembly/development parameters, which are the number of cells required to develop the pack, pack mass, pack volume, and pack cost.

The following conclusions are drawn:

- Both the internal performance parameters and external pack assembly/development parameters showed that the novel prototype 4 Ah cell technology was the optimal technology among all four cell technologies. All cell technologies were tested in depth and subjected to real-world drive cycles, producing very accurate data and results that were used to select the next generation of cell technology for the platform vehicle's prototype battery pack used in RBS.
- The prototype 4 Ah cell technology uses a novel approach to membrane fabrication, where linear nanofibers and microfibers are combined in wet laid nonwoven processes to produce separator membranes. These membranes are strong and thin but have higher porosity (60%–70%) and so have much higher ionic flow compared to membranes of commercial cell technologies used in RBS.
- The results also showed that the prototype 4 Ah cell due to the use of new separator technology features size and capacity comparable to that of other commercial cells and realizes the same output density and durability as capacitors, which makes it a good candidate for the league of high power automotive cells.

CONFLICT OF INTEREST

The authors do not have any conflict of interest.

DATA AVAILABILITY STATEMENT

The data that support the findings of this study are available from the corresponding author, [Mian H. Nazir], upon reasonable request.

ORCID

Mian Hammad Nazir 🔟 https://orcid.org/0000-0002-7623-0625

ENDNOTE

* Due to commercial sensitivity and nondisclosure agreements (NDA), it is not possible to disclose the names of cell technology manufacturers.

REFERENCES

1. Barré A, Deguilhem B, Grolleau S, Gérard M, Suard F, Riu D. A review on lithium-ion battery ageing mechanisms and estimations for automotive applications. *J Power Sources*. 2013;241:680-689.
2. Zuo X, Wu J, Fan C, Lai K, Liu J, Nan J. Improvement of the thermal stability of $LiMn_2O_4$/graphite cells with methylene methanedisulfonate as electrolyte additive. *Electrochim Acta*. 2014;130:778-784.
3. Kucinskis G, Bajars G, Kleperis J. Graphene in lithium ion battery cathode materials: a review. *J Power Sources*. 2013;240: 66-79.
4. Yang Z, Meng Q, Guo Z, Yu X, Guo T, Zeng R. Highly reversible lithium storage in uniform $Li_4Ti_5O_{12}$/carbon hybrid

nanowebs as anode material for lithium-ion batteries. *Energy*. 2013;55:925-932.

5. Kassem M, Bernard J, Revel R, Pélissier S, Duclaud F, Delacourt C. Calendar aging of a graphite/LiFePO₄ cell. *J Power Sources*. 2012;208:296-305.

6. Belt J, Utgikar V, Bloom I. Calendar and PHEV cycle life aging of high-energy, lithium-ion cells containing blended spinel and layered-oxide cathodes. *J Power Sources*. 2011;196(23): 10213-10221.

7. Eddahech A, Briat O, Vinassa J-M. Thermal characterization of a high-power lithium-ion battery: potentiometric and calorimetric measurement of entropy changes. *Energy*. 2013;61:432-439.

8. Maiser E. Battery packaging-technology review. *AIP Conference Proceedings*. Vol. 1597. American Institute of Physics; 2014:204-218.

9. Günther T, Billot N, Schuster J, Schnell J, Spingler FB, Gasteiger HA. The manufacturing of electrodes: key process for the future success of lithium-ion batteries. *Adv Mat Res*. 2016;1140:304-311.

10. Todoroki A, Tanaka Y, Shimamura Y. Delamination monitoring of graphite/epoxy laminated composite plate of electric resistance change method. *Compos Sci Technol*. 2002;62(9): 1151-1160.

11. Nazir MH, Khan ZA, Saeed A. A novel non-destructive sensing technology for on-site corrosion failure evaluation of coatings. *IEEE Access*. 2017;6:1042-1054.

12. Giurgiutiu V. *Structural Health Monitoring of Aerospace Composites*. Elsevier; 2015.

13. Nazir MH, Khan ZA, Saeed A. Experimental analysis and modelling of c-crack propagation in silicon nitride ball bearing element under rolling contact fatigue. *Tribol Int*. 2018;126:386-401.

14. Latif J, Khan ZA, Nazir MH, Stokes K, Plummer J. Life assessment prognostic modelling for multi-layered coating systems using a multidisciplinary approach. *Mater Sci Technol*. 2018;34(6):664-678.

15. Khan ZA, Latif J, Nazir MH, Stokes K, Plummer J. *Sensor based corrosion condition monitoring of coating substrate system informed by fracture mechanics, electrochemistry and heat transfer concepts*. Department of Defense – Allied Nations Technical Corrosion Conference (Paper No. 2017-600147); 2017.

16. Nazir MH, Khan ZA, Saeed A, Stokes K. A predictive model for life assessment of automotive exhaust mufflers subject to internal corrosion failure due to exhaust gas condensation. *Eng Fail Anal*. 2016;63:43-60.

17. Nazir MH, Khan ZA, Stokes K. A holistic mathematical modelling and simulation for cathodic delamination mechanism—a novel and an efficient approach. *J Adhes Sci Technol*. 2015;29:1-39.

18. Nazir MH, Khan Z, Stokes K. Modelling of metal-coating delamination incorporating variable environmental parameters. *J Adhes Sci Technol*. 2014;29(5):392-423.

19. Nazir M, Khan Z, Saeed A, Stokes K. Modelling the effect of residual and diffusion induced stresses on corrosion at the interface of coating and substrate. *Corros Sci*. 2016;72(4):500-517.

20. Nazir MH, Khan ZA, Stokes K. Optimisation of interface roughness and coating thickness to maximise Coating-Substrate adhesion—a failure prediction and reliability assessment modelling. *J Adhes Sci Technol*. 2015;29(14): 1415-1445.

21. Saeed A, Khan ZA, Nazir MH. Time dependent surface corrosion analysis and modelling of automotive steel under a simplistic model of variations in environmental parameters. *Mater Chem Phys*. 2016;178:65-73.

22. Nazir M, Khan ZA, Stokes K. A unified mathematical modelling and simulation for cathodic blistering mechanism incorporating diffusion and fracture mechanics concepts. *J Adhes Sci Technol*. 2015;29(12):1200-1228.

23. Nazir MH, Khan ZA, Stokes K. Analysing the coupled effects of compressive and diffusion induced stresses on the nucleation and propagation of circular coating blisters in the presence of micro-cracks. *Eng Fail Anal*. 2016;70:1-15.

24. Nazir MH, Saeed A, Khan Z. A comprehensive predictive corrosion model incorporating varying environmental gas pollutants applied to wider steel applications. *Mater Chem Phys*. 2017;193:19-34.

25. Nazir M, Khan Z. A review of theoretical analysis techniques for cracking and corrosive degradation of film-substrate systems. *Eng Fail Anal*. 2017;72:80-113.

26. Bajwa R, Khan Z, Nazir H, Chacko V, Saeed A. Wear and friction properties of electrodeposited Ni-Based coatings subject to nano-enhanced lubricant and composite coating. *Acta Metall Sin-Engl*. 2016;29(10):902-910.

27. Nazir MH, Khan Z. Maximising the interfacial toughness of thin coatings and substrate through optimisation of defined parameters. *Int J Comput Meth Exp Meas*. 2015; 3(4):316-328.

28. Bajwa RS, Khan Z, Bakolas V, Braun W. Effect of bath ionic strength on adhesion and tribological properties of pure nickel and Ni-based nanocomposite coatings. *J Adhes Sci Technol*. 2016;30(6):653-665.

29. Bajwa RS, Khan Z, Bakolas V, Braun W. Water-lubricated Ni-based composite (Ni–Al₂O₃, Ni–SiC and Ni–ZrO₂) thin film coatings for industrial applications. *Acta Metall Sin-Engl*. 2015;29(1):8-16.

30. Nazir MH, Khan ZA, Saeed A, et al. Analyzing and modelling the corrosion behavior of Ni/Al₂O₃, Ni/SiC, Ni/ZrO₂ and Ni/Graphene nanocomposite coatings. *Materials*. 2017;10(11):1225.

31. Khan ZA, Grover M, Nazir MH. The implications of wet and dry turning on the surface quality of EN8 steel. In: Yang G-C, Ao S-L, Gelman L, eds. *Transactions on Engineering Technologies*. Springer; 2015:413-423.

32. Khan ZA, Chacko V, Nazir H. A review of friction models in interacting joints for durability design. *Friction*. 2017;5(1):1-22.

33. Khan ZA, Nazir H, Saeed A. Corrosion measurement device. Google Patents. 22 October 2019. https://www.ipo.gov.uk/p-ipsum/Case/ApplicationNumber/GB1719481.2

34. Latif J, Khan ZA, Nazir MH, Stokes K, Smith R. An optimal condition based maintenance scheduling for metal structures based on a multidisciplinary research approach. *Struct Infrastruct Eng*. 2019;15(10):1366-1381.

35. Latif J, Khan ZA, Nazir MH, Stokes K, Plummer J. Condition monitoring and predictive modelling of coating delamination applied to remote stationary and mobile assets. *Struct Health Monit*. 2019;18(4):1056-1073.

36. Savin A, Barsanescu PD, Vizureanu P. Damage detection of carbon reinforced composites using nondestructive evaluation with ultrasound and electromagnetic methods. *IOP Conf Ser Mater Sci Eng*. 2016;133(1):012013.

37. Nazir MH, Khan ZA, Saeed A, Bakolas V, Braun W, Bajwa R. Experimental analysis and modelling for reciprocating wear behaviour of nanocomposite coatings. *Wear*. 2018;416:89-102.

38. Todoroki A, Tanaka M, Shimamura Y. Electrical resistance change method for monitoring delaminations of CFRP laminates: effect of spacing between electrodes. *Compos Sci Technol*. 2005;65(1):37-46.

39. Nazir M, Saeed A, Khan ZA. Electrochemical corrosion failure analysis of large complex engineering structures by using micro-LPR sensors. *Sens Actuators B Chem*. 2018;268:232-244.

40. Lakshmi ND, Kanwar DP, Priya SL. Energy efficient electric vehicle using regenerative braking system. *Int J Adv Ideas Innov Technol*. 2017;3(3):55-58.

41. Lu J, Wu T, Amine K. State-of-the-art characterization techniques for advanced lithium-ion batteries. *Nat Energy*. 2017;2(3):1-13.

42. Lemistre MB, Balageas DL. A hybrid electromagnetic acousto-ultrasonic method for SHM of carbon/epoxy structures. *Struct Health Monit*. 2003;2(2):153-160.

43. Herendeen RA, Ford C, Hannon B. Energy cost of living, 1972–1973. *Energy*. 1981;6(12):1433-1450.

44. Adhikary D, Rahman MZ, Nahin MM, Bin Abdullah MS. Design and implementation of regenerative braking system. *Smart Materials, Adaptive Structures and Intelligent Systems*. ASME 2013 Conference on Smart Materials, Adaptive Structures and Intelligent Systems, September 16-18, 2013, Snowbird, UT; 2013.

45. Clegg S. *A Review of Regenerative Braking Systems*. Institute of Transport Studies, University of Leeds; 1996. Working Paper 471.

46. Fletcher R. Regenerative equipment for railway rolling stock. *Power Eng J*. 1991;5(3):105-114.

47. Tomaszewska A, Chu Z, Feng X, et al. Lithium-ion battery fast charging: a review. *eTransportation*. 2019;1:100011.

48. Shi M, Tai Z, Li N, et al. Spherical graphite produced from waste semi-coke with enhanced properties as an anode material for li-ion batteries. *Sustain Energy Fuels*. 2019;3(11):3116-3127.

49. Chen Y-H, Wang C-W, Liu G, Song X-Y, Battaglia V, Sastry AM. Selection of conductive additives in Li-ion battery cathodes: a numerical study. *J Electrochem Soc*. 2007;154(10):A978.

50. Kim JK, Kim DH, Joo SH, et al. Hierarchical chitin fibers with aligned nanofibrillar architectures: a nonwoven-mat separator for lithium metal batteries. *ACS Nano*. 2017;11(6):6114-6121.

51. Hubbe MA, Koukoulas AA. Wet-laid nonwovens manufacture–chemical approaches using synthetic and cellulosic fibers. *BioResources*. 2016;11(2):5500-5552.

52. Zhang H, Zhou M-Y, Lin C-E, Zhu B-K. Progress in polymeric separators for lithium ion batteries. *RSC Adv*. 2015;5(109):89848-89860.

53. Ding L, Zhang C, Wu T, Yang F, Cao Y, Xiang M. The compression behavior, microstructure evolution and properties variation of three kinds of commercial battery separators under compression load. *J Power Sources*. 2020;451:227819.

54. Lee H, Yanilmaz M, Toprakci O, Fu K, Zhang X. A review of recent developments in membrane separators for rechargeable lithium-ion batteries. *Energy Environ Sci*. 2014;7(12):3857-3886.

55. Lagadec MF, Zahn R, Wood V. Characterization and performance evaluation of lithium-ion battery separators. *Nat Energy*. 2019;4(1):16-25.

56. Chen L, Fan X, Hu E, et al. Achieving high energy density through increasing the output voltage: a highly reversible 5.3 V battery. *Chem*. 2019;5(4):896-912.

57. Liu C, Koyyalamudi BB, Li L, Emani S, Wang C, Shaw LL. Improved capacitive energy storage via surface functionalization of activated carbon as cathodes for lithium ion capacitors. *Carbon*. 2016;109:163-172.

58. Musolino V, Tironi E, di Milano P. *A comparison of supercapacitor and high-power lithium batteries*. IEEE Conference on Electrical Systems for Aircraft, Railway and Ship Propulsion. October 19-21, 2010;2010:1-6.

59. Toyota boshoku report 2018. Accessed August 11, 2021. https://www.toyota-boshoku.com/global/content/wp-content/uploads/TBreportE_2018.pdf

60. Kostecki R, Norin L, Song X, McLarnon F. Diagnostic studies of polyolefin separators in high-power li-ion cells. *J Electrochem Soc*. 2004;151(4):A522.

61. Liu R, Yuan B, Zhong S, et al. Poly (vinylidene fluoride) separators for next-generation lithium based batteries. *Nano Select*. 2021;2(12):2308-2345.

62. Bitrode SL Corporation. Accessed August 24, 2022. https://www.bitrode.com/model-mcv/

63. International Electrotechnical Commission. *Secondary Lithium-ion Cells for the Propulsion of Electric Road Vehicles-Part 1: Performance Testing*. International Electrotechnical Commission; 2010.

64. Wright RB, Christophersen JP, Motloch CG, et al. Power fade and capacity fade resulting from cycle-life testing of advanced technology development program lithium-ion batteries. *J Power Sources*. 2003;119:865-869.

65. Dees D, Gunen E, Abraham D, Jansen A, Prakash J. Electrochemical modeling of lithium-ion positive electrodes during hybrid pulse power characterization tests. *J Electrochem Soc*. 2008;155(8):A603.

66. Yazami R, Reynier YF. Mechanism of self-discharge in graphite–lithium anode. *Electrochim Acta*. 2002;47(8):1217-1223.

67. dataTaker Intelligent Data Loggers. *DT85 series 4 data logger intelligent data logging products*. Accessed October 16, 2020. http://www.datataker.com/

68. Eddahech A, Briat O, Bertrand N, Deletage J-Y, Vinassa J-M. Behavior and state-of-health monitoring of li-ion batteries using impedance spectroscopy and recurrent neural networks. *Int J Electr Power Energy Syst*. 2012;42(1):487-494.

69. Perdana FA, Supriyanto A, Purwanto A, Jamaluddin A. Study of imbalanced internal resistance on drop voltage of $LiFePO_4$ battery system connected in parallel. *J Phys Conf Ser*. 2017;795(1):012036.

70. Liu Z, Onori S, Ivanco A. Synthesis and experimental validation of battery aging test profiles based on real-world duty cycles for 48-V mild hybrid vehicles. *IEEE Trans Veh Technol*. 2017;66(10):8702-8709.

71. Siczek KJ. Chapter one—basic concepts. In: Siczek KJ, ed. *Next-Generation Batteries with Sulfur Cathodes*. Academic Press; 2019:1-4.

72. Aelterman P, Rabaey K, Pham HT, Boon N, Verstraete W. Continuous electricity generation at high voltages and currents using stacked microbial fuel cells. *Environ Sci Technol*. 2006;40(10):3388-3394.

73. Barai A, Uddin K, Dubarry M, et al. A comparison of methodologies for the non-invasive characterisation of commercial li-ion cells. *Prog Energy Combust Sci*. 2019;72:1-31.

74. Barai A, Uddin K, Widanalage W, McGordon A, Jennings P. The effect of average cycling current on total energy of lithium-ion batteries for electric vehicles. *J Power Sources.* 2016;303:81-85.

75. Yang S, Deng C, Zhang Y, He Y. State of charge estimation for lithium-ion battery with a temperature-compensated model. *Energies.* 2017;10(10):1560.

76. Anseán D, García V, González M, Viera J, Blanco C, Antuña J. DC internal resistance during charge: analysis and study on LiFePO$_4$ batteries. 2013 World Electric Vehicle Symposium and Exhibition (EVS27); 2013:1–11.

77. Yang F, Lu L, Yang Y, He Y. Characterization, analysis and modeling of an ultracapacitor. *World Electric Vehicle Journal.* 2010;4(2):358-369.

78. Molaeimanesh G, Mousavi-Khoshdel S, Nemati A. Experimental analysis of commercial LiFePO$_4$ battery life span used in electric vehicle under extremely cold and hot thermal conditions. *J Therm Anal Calorim.* 2021;143:3137-3146.